05,08,09

Nature of defects responsible for the red shift of the fundamental absorption edge and the increase in the refractive index of irradiated Si_3N_4

© V.A. Gritsenko [1,2], Yu.N. Novikov [1,¶], A.A. Gismatulin [1]

[1] Rzhanov Institute of Semiconductor Physics, Siberian Branch, Russian Academy of Sciences, Novosibirsk, Russia
[2] Novosibirsk State Technical University, Novosibirsk, Russia
¶ E-mail: nov@isp.nsc.ru

Received October 17, 2025
Revised November 5, 2025
Accepted November 5, 2025

The atomic structure of amorphous silicon nitride Si_3N_4 irradiated with boron (B^+) ions is studied using photoelectron spectroscopy and infrared absorption. Irradiation with B^+ ions is accompanied by a red shift of the fundamental absorption edge of Si_3N_4. Irradiation with B^+ ions leads to a broadening of the Si 2s atomic level toward lower energies, indicating the formation of Si 2*s* bonds. The formation of Si−Si bonds due to the splitting of bonding and antibonding orbitals leads to a decrease in the bandgap and an increase in the refractive index.

Keywords: silicon nitride, Si_3N_4, fundamental absorption edge, refractive index, Si−Si bonds.

DOI: 10.61011/PSS.2025.11.62960.281-25

1. Introduction

Amorphous silicon oxide (SiO_2) and amorphous silicon nitride (Si_3N_4) are two key dielectrics in microelectronics [1]. Thermal SiO_2 on silicon has low density of traps on the surface and in the volume, and is therefore used as a gate dielectric in MIS-transistors [1]. At the same time, Si_3N_4 has high concentration ($10^{18}-10^{21}\,cm^{-3}$) of deep ($\approx 1.5\,eV$) electron and hole traps [1–3], which may capture a charge and store it for ten years at 85 °C. This effect is used in the modern flash memory based on TANOS-structures ($TaN-Al_2O_3-Si_3N_4-SiO_2-Si$) [4,5]. Electron and hole traps considered in Si_3N_4 are various defects: dangling bonds of silicon and nitrogen [6,7], silicon-silicon bond (Si−Si bond) [8–11] etc. To understand and optimize the operation of the flash memory, it is important to know the nature of traps in Si_3N_4.

Paper [12] found that the fundamental absorption edge in Si_3N_4 radiated with neon ions moved towards lower energies in $0.5-1.0\,eV$ depending on the synthesis technology. Annealing of Si_3N_4 at 700 °C causes reverse shift of the absorption edge towards higher energies. In article [12] it is specified that the shift of the absorption edge in radiation is due to the disordering of the silicon nitride structure. In paper [13] the processes of charge accumulation/drain were studied in silicon nitride radiated with boron and phosphorus ions. The nature of the defects arising from radiation in papers [12,13], was not studied.

The aim of this paper is to establish the nature of defects in radiated Si_3N_4 with B^+ ions influencing the optical properties Si_3N_4 — fundamental absorption edge and refractive index.

2. Experimental procedure

Amorphous films Si_3N_4 are synthesized from silane SiH_4 and ammonia NH_3 mix at temperature of 850 °C at the ratio of $SiH_4/NH_3 = 1/100$. Si_3N_4 was radiated with B^+ ions with energy of 100 keV and with dose of $3 \cdot 10^{14}\,cm^{-2}$. Annealing of the radiated Si_3N_4 was carried out in the nitrogen atmosphere at temperature of 700 °C for 30 min. To study the photoelectron spectra, Si_3N_4 films with thickness of 100 nm were deposited on silicon of *n*-type with orientation of (100). X-ray photoelectron spectra were measured using an X-ray photoelectron spectrometer (XPS) SPECS with monochromatic radiation Al K_α ($E = 1486.74\,eV$). For optical measurements, Si_3N_4 was deposited onto sapphire substrates. The thickness and the refractive index of Si_3N_4 films were measured using an ellipsometer at wavelength of 632.8 nm. Optical spectra of reflection and transmittance were measured in an SF-56 spectrometer (LOMO-Spektr, Saint Petersburg, Russia). The infrared spectra of transmittance were measured in a Fourier transform spectrometer FT-801 (SIMEX, Russia).

3. Distribution of boron and defects in radiated Si_3N_4

The distribution of implanted B^+ in the Si_3N_4/Si-substrate system was calculated out using STRIM-2013 software. The following parameters were used in calculation: thickness of Si_3N_4 100 nm with density of $3.44\,g/cm^3$, Si-substrate thickness of 400 nm. The implantation of 1000 B^+ ions with energy of 100 keV was calculated. The implantation angle was 0 degrees. The calculation results are presented

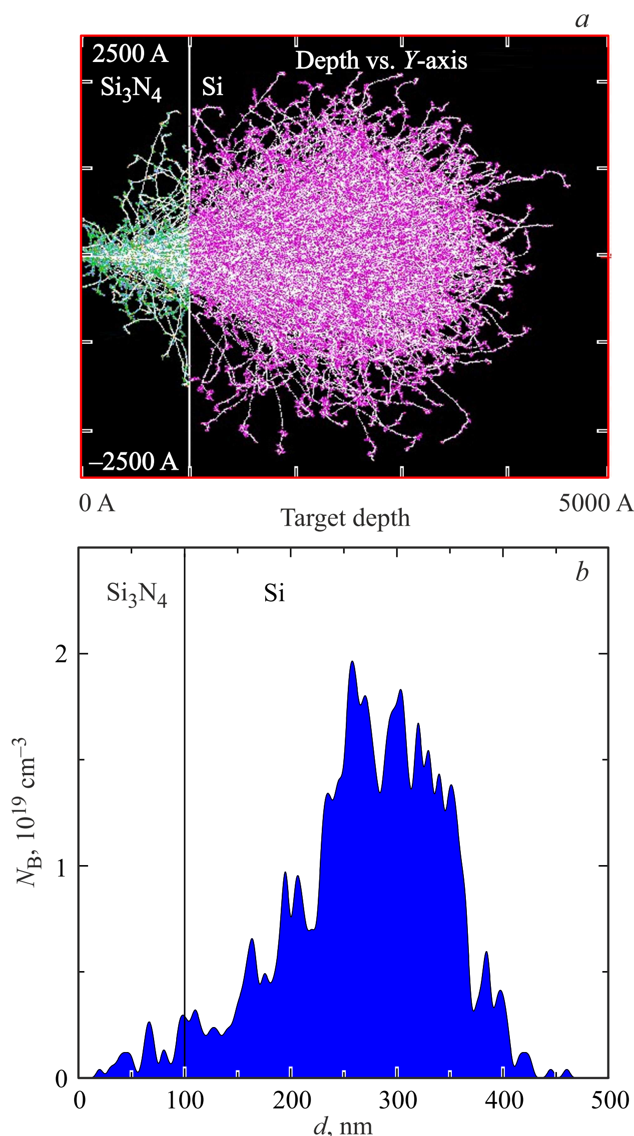

Figure 1. *a* — estimated tracks of 1000 B^+ ions in Si_3N_4/Si structure (white color). Collision of B^+ with nitrogen in Si_3N_4 (green color). Collision of B^+ ions with Si in a substrate (pink color); *b* — spatial distribution of B^+ ions in Si_3N_4 after ion implantation. Implantation energy is 100 keV, implantation dose is $3 \cdot 10^{14}\,cm^{-2}$.

in Figure 1. The calculated tracks of boron ions after implantation are shown in Figure 1, *a*. Figure 1, *b* shows spatial distribution of B^+ ions in Si_3N_4 after ion implantation with energy of 100 keV at implantation dose of $3 \cdot 10^{14}\,cm^{-2}$. From distribution of B^+ ions in Si_3N_4 after ion implantation (Figure 1, *b*) you can see that the main part of B^+ ions goes into the silicon substrate.

4. Optical properties of radiated Si_3N_4

Transmittance spectra Si_3N_4 on a sapphire substrate, before and after radiation with B^+ ions are shown in Figure 2.

Radiation with B^+ ions is accompanied with reduction in transmittance of radiated Si_3N_4 in the energy range of 3.5–6.0 eV. Spectral dependence of fundamental absorption edge in the source and radiated film Si_3N_4 is shown in Figure 3. Dispersion spectra of α optical absorption make it possible to estimate the value of the band gap as the energy of photon, at which α is $10^4\,cm^{-1}$ (so called optical slit E_{04}) (Figure 3). You can see that for the source and radiated films with doses of $3 \cdot 10^{14}\,cm^{-2}$, the values E_{04} are 5.2 and 4.8 eV accordingly.

A similar low energy shift of fundamental absorption edge is observed when the nonstoichiometric SiN_x is enriched with silicon [14,15]. Besides, we also calculated the spectra of optical absorption (solid lines in Figure 3) using Urbach rule [16]: $\alpha = \alpha_0 \exp\big((\hbar\omega - E_{04})/E_U\big)$, where α_0 and E_U (Urbach energy) are model parameters. The agreement with the experiment was obtained at the following parameters: $\alpha_0 = 9.7 \cdot 10^3\,cm^{-1}$, $E_U = 0.39$ eV at $E_{04} = 5.2$ eV; $E_U = 0.55$ eV at $E_{04} = 4.8$ eV. The calculations show that with the increase of the radiation dose Si_3N_4 using B^+ ions, the value E_U increases. Increase of E_U certifies the increase of disorder in the B^+ ion radiated Si_3N_4. Therefore, as the dose of silicon nitride film radiation with B^+ ions increases, the optical absorption edge shifts into the long-wavelength area of the spectrum. Previously, the low-energy shift of the fundamental absorption edge was observed in radiation of silicon nitride with neon ions and protons [12].

Reflection spectra of Si_3N_4 radiated with B^+ ions on silicon are shown in Figure 4.

The refractive index of the silicon substrate is more than in Si_3N_4 film. In this case the minimum reflection (from the reflecting coating) corresponds to the minimum thickness

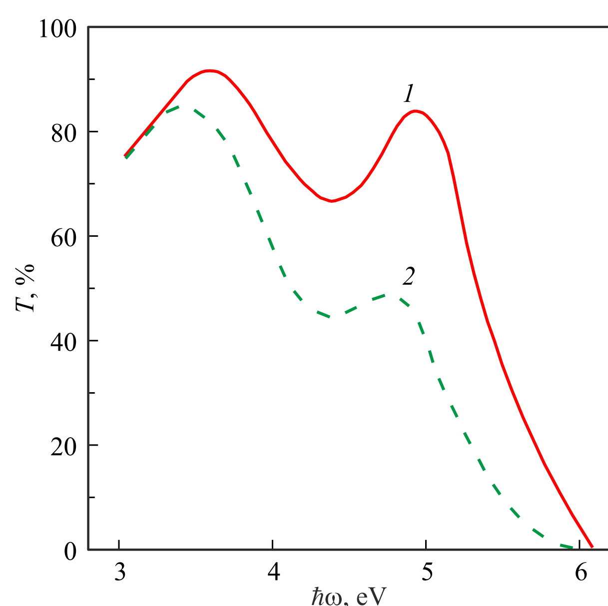

Figure 2. Transmittance spectra Si_3N_4 on a sapphire substrate: *1* — source Si_3N_4, *2* — after radiation with B^+ ions at dose of $3 \cdot 10^{14}\,cm^{-2}$.

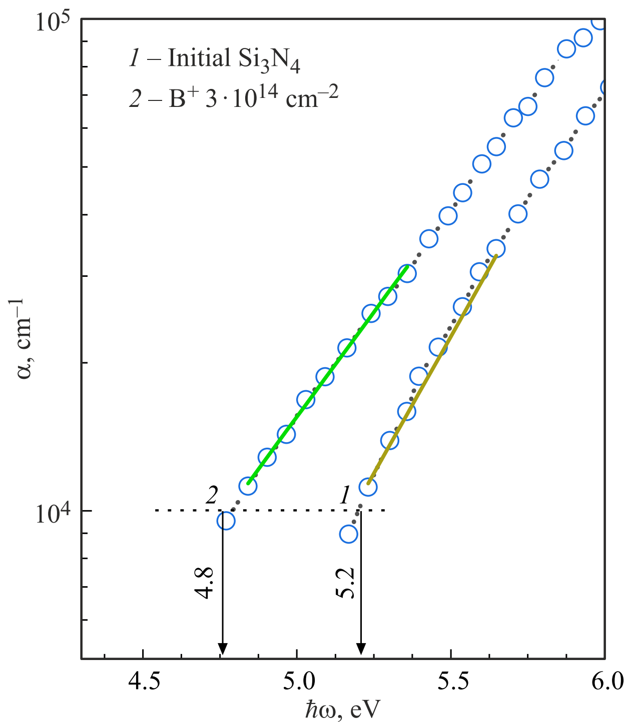

Figure 3. Spectral dependence of absorption coefficient Si_3N_4, *1* — source and *2* — after radiation with B^+ ions (circles). Solid lines — spectral dependence of absorption coefficient Si$-$3N$_4$ calculated using Urbach rule.

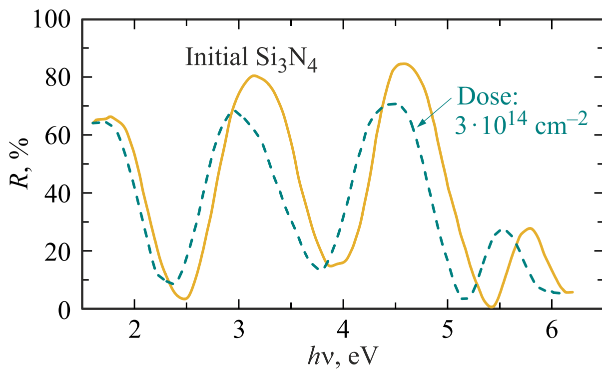

Figure 4. Reflection spectra of Si_3N_4 radiated with B^+ ions on a silicon substrate: solid line — source Si_3N_4, dotted line — Si_3N_4 after implantation of B^+ ions with energy of 100 keV at the dose of $3 \cdot 10^{14}$ cm^{-2}.

equal to one quarter of the wavelength:

$$n(\lambda)d = \frac{m + 1/2}{2}\lambda, \quad (1)$$

maximum in reflection (minimum in transmittance):

$$n(\lambda)d = \frac{m}{2}\lambda, \quad (2)$$

where λ — wavelength, m — order of interference, d — thickness Si_3N_4, determined by us using ellipsometry. Oscillations of the reflection coefficient are caused by interference.

Spectral dependence of the refractive index Si_3N_4, radiated with B^+ ions, is shown in Figure 5. Radiation of Si_3N_4 with B^+ ions causes vertical shift of spectrum $n(\hbar\omega)$ to the area of high values. Increase of the radiation dose is accompanied with the increased refractive index similarly to what is observed in the enrichment of the nonstoichiometric SiN_x with excessive silicon [17]. Increase of the refractive index of the film as a result of radiation is caused by appearance of high concentration of Si$-$Si bonds in Si_3N_4 film, which is equivalent to the formation of nonstoichiometric silicon nitride SiN_x enriched with silicon.

Spectra of infrared transmittance of the radiated Si_3N_4 on the silicon substrate before and after annealing are shown in Figure 6. Stretching vibrations of Si$-$N bond have minimum transmittance near 850 cm^{-1} ($\approx 12\,\mu$m). Upon radiation of Si_3N_4 with B^+ ions the transmittance parameter increases at 850 cm^{-1}.

Increased intensity of infrared absorption of stretching vibrations of Si$-$N bonds in Si_3N_4, implanted with B^+ ions (see Figure 6) specifies a break of Si$-$N bonds by reaction:

$$\equiv\text{Si}-\text{N}= \rightarrow \equiv\text{Si}\cdot + \cdot\text{N}= . \quad (3)$$

As a result of the break of $\equiv$Si$-$N$=$ bond, a paramagnetic triple-coordinated silicon atom is formed with an unpaired electron $\equiv$Si$\cdot$ and a paramagnetic double-coordinated nitrogen atom with an unpaired electron $\cdot$=N$\cdot$. From Figure 6 it

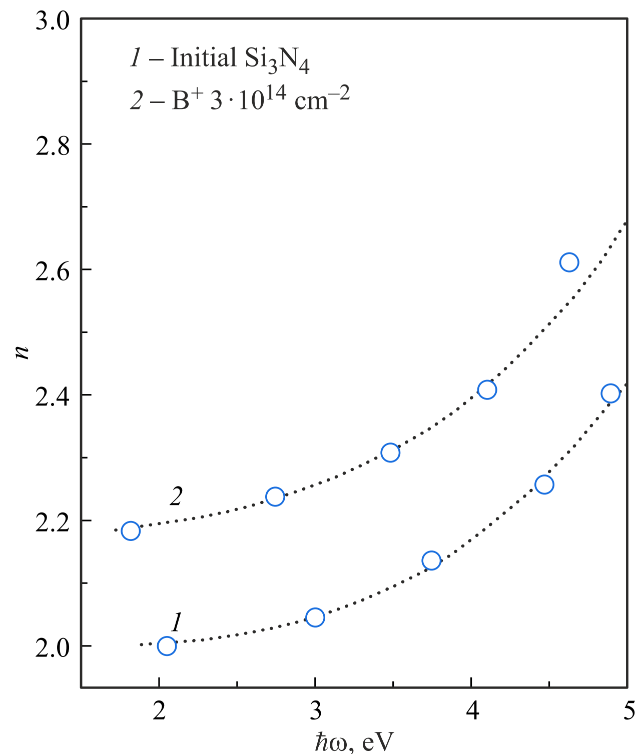

Figure 5. Spectral dependence of refractive index n Si_3N_4: *1* — before radiation, *2* — after radiation with B^+ ions with dose of $3 \cdot 10^{14}$ cm^{-2}.

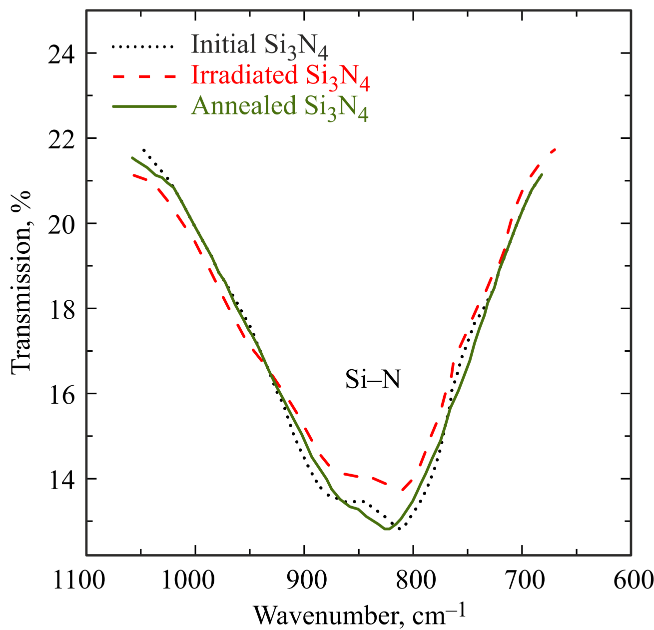

Figure 6. Spectrum of infrared transmittance of source films Si_3N_4 and Si_3N_4, radiated with B^+ ions (dose $3 \cdot 10^{14}\,cm^{-2}$) before and after the subsequent annealing.

follows that upon radiation of Si_3N_4 with B^+ ions, around one percent of Si–N bonds is broken by reaction (3). Annealing is accompanied with spectra return to the source state (Figure 6). Such behavior of infrared spectra of transmittance may be explained by a break of Si–N bonds upon radiation of Si_3N_4 and subsequent recovery of Si–N bonds in annealing.

5. Photoelectron spectroscopy of radiated Si_3N_4

Figure 7 presents experimental photoelectron spectra of Si $2s$ states for Si, Si_3N_4, implanted with B^+ ions and source Si_3N_4. Radiation with B^+ Si_3N_4 ions is accompanied with broadening and shift of Si $2s$ spectrum towards lower energies (Figure 7). For expansion of Si $2s$ spectra it was presumed that five tetrahedrons $SiN_\nu Si_{4-\nu}$ (where $\nu = 0$, 1, 2, 3, 4) contribute to spectrum of Si $2s$ state, and these contributions are presented as a sum of Gaussian and Lorenz functions (GL) [18].

First the energy position (E_ν) and width (σ_ν) of Si $2s$ state were defined for Si (tetrahedron $SiSi_4$) — $E_0 = 151$ eV and $\sigma_0 = 2$ eV [19] and Si_3N_4 (tetrahedron SiN_4) — $E_4 = 152.6$ eV and $\sigma_4 = 2.8$ eV [20]. Positions and widths of three intermediate functions of GL states Si $2s$ (E_ν and σ_ν, where $\nu = 1, 2, 3$) for tetrahedrons $SiNSi_3$, SiN_2Si_2 and $SiNSi_3$ were determined by linear interpolation of $E_0(\sigma_0)$, $E_4(\sigma_4)$ values using the number of silicon atoms as a parameter. Expansion of Si $2s$ spectra in Figure 7, which are shown with solid lines, was done using equation [18]:

$$I(E) = \sum_{\nu=4}^{4} W_\nu \left[(1-\chi)\exp\left(\frac{-4\ln(2)(E-E_\nu)^2}{\sigma_\nu^2}\right) + \frac{\chi}{1 + 4\frac{(E-E_\nu)^2}{\sigma_\nu^2}} \right], \quad (4)$$

where $I(E)$ — estimated spectrum, E — energy, χ — parameter of GL function mixing, W_ν — contribution to spectrum Si $2s$ of $SiN_\nu Si_{4-\nu}$ ($\nu = 0$, 1, 2, 3, 4) tetrahedrons. Values of W_ν were selected from the best agreement of the experimental and estimated spectra. Value of $\chi = 0.6$ for radiated Si_3N_4 and Si, and $\chi = 0.75$ for source Si_3N_4. Expansion of spectrum Si $2s$ Si_3N_4, radiated with B^+ ions, demonstrated that the main contribution to spectrum Si $2s$ is made by $SiSi_4$, $SiSi_3N$ and SiN_4 tetrahedrons (Figure 7). The estimate shows that the broadening of level Si $2s$ when radiated with B^+ ions is related to formation of Si–Si bonds in Si_3N_4.

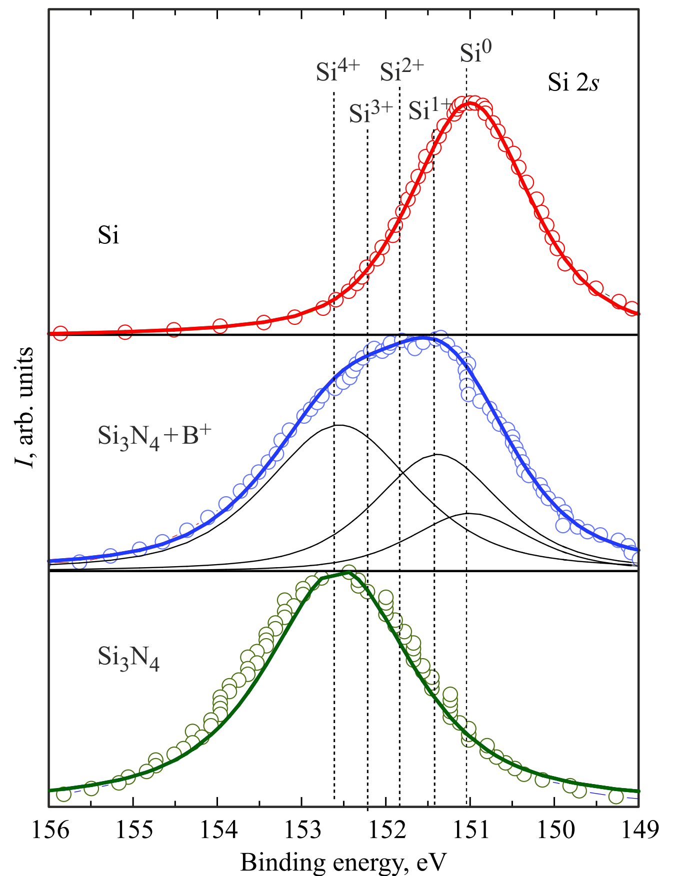

Figure 7. Experimental XPS-spectra of the level (circles) of the ion implanted Si, the source film Si_3N_4 and the result of their expansion (solid lines). Designations Si^{4+}, Si^{3+}, Si^{2+}, Si^{1+} and Si^0 indicate the contributions to spectrum Si $2s$ from five tetrahedrons $SiN_\nu Si_{4-\nu}$, where $\nu = 0, 1, 2, 3, 4$.

6. Discussion of results

Radiation of Si_3N_4 with B^+ ions is accompanied with low energy shift of the fundamental absorption edge and increase of the refractive index. As a result of a break of $\equiv$Si$-$N$=$ bond upon radiation, according to reaction (2), two internal paramagnetic complementary defects are formed: triple-coordinated silicon atom with an unpaired electron $\equiv$Si and double-coordinated nitrogen atom with an unpaired electron $=$N. This is confirmed by the decrease in the absorption coefficient of oscillatory spectra in the infrared area of the spectrum. In paper [21] it is shown that the enrichment of the silicon nitride with excessive silicon causes increased absorption coefficient and decreased band gap value. Increase of the refractive index and low energy shift of the fundamental absorption edge of radiated Si_3N_4 are caused by formation of Si$-$Si bonds. Formation of Si$-$Si bonds in radiated Si_3N_4 is indirectly indicated by broadening of the atomic level of Si $2s$ and spectrum displacement to the area of low energies, i. e. towards the silicon states.

After radiation of Si_3N_4 the paramagnetic defects $\equiv$Si and $=$N are recombined in pairs according to the following reactions:

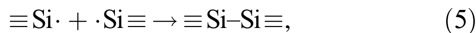

$$\equiv \text{Si}\cdot + \cdot\text{Si}\equiv \rightarrow \equiv \text{Si–Si}\equiv, \quad (5)$$

$$= \text{N}\cdot + \cdot\text{N} = \rightarrow = \text{N–N} = . \quad (6)$$

As a result of recombination of paramagnetic defects $\equiv$Si$\cdot$ and $=$N$\cdot$ in the radiated Si_3N_4 the diamagnetic bonds Si$-$Si and N$-$N are formed. Formation of Si$-$Si bonds causes narrowing of the band gap width (Figure 8). Decrease of the band gap width with increased enrichment of SiN_x with silicon was observed in papers [22,23]. The top of the valence band SiN_x is mainly formed with atomic Si $3p$-orbitals, corresponding to binding σ-orbitals of Si$-$Si bonds, and the shift of E_V towards higher energies is explained by the increased energy of these orbitals with the growth of nitrogen vacancy concentration (Figure 8).

As quantum-chemical estimates of the electron structure show, the shift of the absorption edge SiN_x is caused by the shift of the conduction band edge E_C and the valence band ceiling E_V to the band gap [8,10,11]. Binding and loosening orbitals of Si$-$Si bond are located near the valence band ceiling and conduction band bottom of Si_3N_4. Shift of E_C and E_V in the direction of the band gap causes low energy shift of the fundamental absorption edge. In other words, the increase of concentration of Si$-$Si bonds in process of radiation, as a result of degeneracy removal, causes decrease in the width of the silicon nitride band gap (Figure 8).

The Si refractive index in the IR-area of the spectrum is ≈ 3.9 [24], and the refractive index of Si_3N_4 is ≈ 2 [25]. Therefore, the increase in the number of Si$-$Si bonds in SiN_x causes the increase of the refractive index (Figure 5). Upon annealing of the radiated Si_3N_4 the interaction of Si$-$Si and N$-$N bonds occurs according to the following reaction:

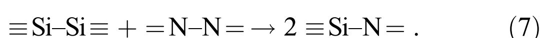

$$\equiv \text{Si–Si}\equiv + = \text{N–N} = \rightarrow 2 \equiv \text{Si–N} = . \quad (7)$$

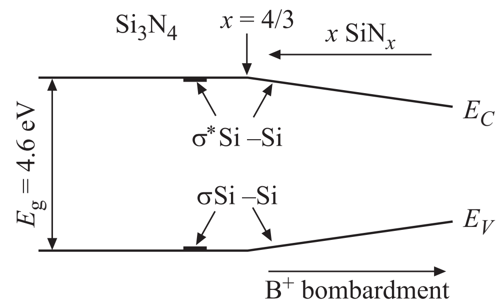

Figure 8. Schematic image of decreased width of band gap SiN_x and radiated Si_3N_4 due to formation of Si$-$Si bonds in process of radiation.

This is confirmed by the decrease in the transmittance coefficient of radiated Si_3N_4 in the infrared area of the spectrum at wavelength $850\,\text{cm}^{-1}$ in process of annealing (Figure 6).

7. Conclusion

The effect of radiation with B^+ ions on the structure and optical properties of amorphous Si_3N_4 was studied. Radiation with B^+ ions causes a shift in the fundamental absorption edge to the red area of the spectrum and increased refractive index Si_3N_4. The subsequent annealing causes disappearance of radiation-induced effects in the radiated Si_3N_4.

Funding

The study was supported by the state assignment of the Institute of Semiconductor Physics, Siberian Branch, Russian Academy of Sciences No. FWGW-2025-0010.

Conflict of interest

The authors declare that they have no conflict of interest.

References

[1] V.A. Gritsenko, Stroenie i elektronnaya struktura amorfnykh dielektrikov v kremnievykh MDP strukturakh. Nauka, M. (1993). 278 s. (in Russian).

[2] L. Hückmann, J. Cottom, J. Meyer. Adv. Phys. Res. **3**, 2300109 (2024).

[3] C. Wilhelmer, D. Waldhör, L. Cvitkovich, D. Milardovich, M. Waltl, T. Grasse. Phys. Rev. B **110**, 045201 (2024).

[4] A. Goda. Electronics **10**, 3156 (2021).

[5] A. Padovani, A. Arreghini, L. Vandelli, L. Larcher, G. Van den bosch, P. Pavan, J. Van Houdt. IEEE Trans. Electron Devices **58**, 3147 (2011).

[6] W.L. Warren, P.M. Lenahan. Phys. Rev. B **42**, 1773 (1990).

[7] W.L. Warren, P.M. Lenahan, S.E. Curry. Phys. Rev. Lett. **65**, 207 (1990).

[8] A.A. Karpushin, A.N. Sorokin, V.A. Gritsenko. JETP Letters **103**, *3*, 171 (2016).

[9] V.A. Gritsenko, T.V. Perevalov, O.M. Orlov, G.Ya. Krasnikov. Appl. Phys. Lett. **109**, 06294 (2016).
[10] L. Martín-Moreno, E. Martínez, J.A. Vergés, F. Yndurain. Phys. Rev. B **35**, 9683 (1987).
[11] J.F. Justo, F. de Brito Mota, A. Fazzio. Phys. Rev. B **65**, 073202 (2002).
[12] H.J. Stein. J. Appl Phys. **47**, *8*, 3421 (1976).
[13] G. Li, H. San, X.-Y. Chen. J. Appl. Phys. **105**, 124503 (2009).
[14] O. Debieu, R.P. Nalini, J. Cardin, X. Portier, J. Perriére, F. Gourbilleau. Nanoscale Res. Lett. **8**, 31 (2013).
[15] R. Karcher, L. Ley, R.L. Johnson. Phys. Rev. **8**, *30*, 1896 (1984).
[16] O.V. Rambadey, A. Kumar, A. Sati, P.R. Sagdeo. ACSOmega **6**, 32231 (2021).
[17] F. Tiour, B. Benyahia, N. Brihi, A. Sari, Br. Mahmoudi, A. Manseri, A. Guenda. Appl. Phys. A **126**, (2020) 59.
[18] V. Jaina, M.C. Biesingerb, M.R. Linford. Appl. Surf. Sci. **447**, 548 (2018).
[19] http://xpsdatabased/silicon-si-z14
[20] I. Hoflijk, A. Vanleenhove, I. Vaesen, C. Zborowski, K. Artyushkova, T. Conard. Surf. Sci. Spectra **29**, 014013 (2022).
[21] G. Heinricha, I. Höger, M. Bähr, K. Stolberg, T. Wütherich, M. Leonhardt, A. Lawerenz, G. Gobsch. Energy Procedia **27**, 491 (2012).
[22] H.H. Nguyen, R. Jayapal, N.S. Dang, V.D. Nguyen, T.T. Trinh, K. Jang, J. Yi. Microelectron. Eng. **98**, 34 (2012).
[23] I. Guler. ECS J. Solid State Sci. Technol. **12**, 046002 (2023).
[24] https://refractiveindex.info/?shelf=main&book=Si&page=Schinke.
[25] https://en.wikipedia.org/wiki/Silicon_nitride.

Translated by M.Verenikina